NAA-SR-4528
REACTORS-GENERAL
42 PAGES

RESULTS OF HIGH-TEMPERATURE STRAIN-FATIGUE TESTS ON REACTOR-GRADE ALUMINUM-BASE MATERIALS

By
W. F. ANDERSON
W. WAHL

ATOMICS INTERNATIONAL
A DIVISION OF NORTH AMERICAN AVIATION, INC.
P.O. BOX 309 CANOGA PARK, CALIFORNIA

CONTRACT: AT(11-1)-GEN-8
ISSUED: JAN 30 1961

DISTRIBUTION

This report has been distributed according to the category "Reactors-General" as given in "Standard Distribution Lists for Unclassified Scientific and Technical Reports" TID-4500 (15th Ed.), August 1, 1959. A total of 625 copies were printed.

ACKNOWLEDGMENT

Testing of the specimens was carried out by C. R. Waldron of the Missile Division of North American Aviation, Inc. J. A. Roberson performed the metallographic examination of the material and failed specimens.

CONTENTS

		Page
	Abstract	v
I.	Introduction	1
II.	Test Machine Operation	2
	A. General Description	2
	B. Plastic Strain Calibration	2
III.	Test Results	10
	A. Material Tested	10
	B. Strain-Fatigue Test Results	11
	C. Results of Metallographic Examination	15
IV.	Discussion of Results	28
	A. Temperature, Ductility, and Cyclic-Life Relations	28
	B. Interpretation of Plastic Strain	20
V.	Conclusions	32
	Appendix	33
	References	36

TABLES

I.	Chemical Analyses of Specimen Material	11
II.	Mechanical Properties of Specimen Material	12
III.	Constants "k" and "C" for Formula $N^k = C\epsilon_p$	30

FIGURES

1.	Plastic-Strain-Calibration and Fatigue Test Specimens	4
2.	Typical Sanborn Record of Deflection and Load	5
3.	Stress vs Strain Mechanical Hysterisis Loop for 1132 Reactor-Grade Aluminum at 600°F	6
4.	Stress vs Strain Mechanical Hysterisis Loop for Alcoa M-257 at 900°F	7
5.	Plastic Strain vs Total Strain for 1132 Reactor-Grade Aluminum	8
6.	Plastic Strain vs Total Strain for Alcoa M-257	9

FIGURES

		Page
7.	Strain Range vs Cycles to Failure for 1197 Reactor-Grade Aluminum	13
8.	Strain Range vs Cycles to Failure for 1132 Reactor-Grade Aluminum	13
9.	Strain Range vs Cycles to Failure for Alcoa M-257	13
10.	One-half Total Stress Range vs Cycles to Failure for 1197 Reactor-Grade Aluminum	14
11.	One-half Total Stress Range vs Cycles to Failure for 1132 Reactor-Grade Aluminum	14
12.	One-half Total Stress Range vs Cycles to Failure for Alcoa M-257	14
13.	Plastic Strain vs Cycles to Failure for 1197 Reactor-Grade Aluminum	15
14.	Plastic Strain vs Cycles to Failure for 1132 Reactor-Grade Aluminum	16
15.	Plastic Strain vs Cycles to Failure for Alcoa M-257	17
16.	Cycles to Failure and Elongation vs Test Temperature for Alcoa M-257	18
17.	Structure of Alcoa M-257 Samples	20
18.	Fracture of Alcoa M-257 Sample	20
19.	Structure of Three Samples of 1132 Reactor-Grade Aluminum	21
20.	Fracture of Three Samples of 1132 Reactor-Grade Aluminum	21
21.	Microstructure of 1132 Sample Fatigued at 80°F	22
22.	Microstructure of 1132 Sample Fatigued at 300°F	22
23.	Microstructure of 1132 Sample Fatigued at 600°F	23
24.	Structure of Three Samples of 1197 Reactor-Grade Aluminum	23
25.	Fracture of Four Samples of 1197 Reactor-Grade Aluminum	24
26.	Microstructure of 1197 Sample Fatigued at 80°F	25
27.	Microstructure of 1197 Sample Fatigued at 80° F	25
28.	Microstructure of 1197 Sample Fatigued at 300°F	26
29.	Microstructure of 1197 Sample Fatigued at 600°F	27

ABSTRACT

Strain-fatigue tests were conducted on two reactor-grade aluminum-base alloys and a sintered-aluminum product at temperatures ranging from 80 to 900°F. These materials are used in reactor components, and one of the alloys, the high-purity aluminum, has a potential for use in experimental models. Results of the tests indicate strain-fatigue behavior at room temperature for all three materials was similar to that of other ductile materials. The aluminum-alloy specimens, at 600°F test temperature, yielded results of limited value due to instability of the specimens. At 900°F, the sintered-aluminum product exhibited a significant loss of ductility, with a cyclic life 16% of that at 600°F.

I. INTRODUCTION

This report covers part of a program under AEC auspices, aimed at obtaining and presenting data for use in design of nuclear reactors. The program includes studies of structural, cladding, and fuel materials in their normal state and with their properties impaired by fabrication procedures or exposure to various environments.

The aim of this investigation was to obtain and present data useful for analytical prediction of cyclic temperature service life of components fabricated from aluminum-base materials. Three materials were selected as characteristic of aluminum-base materials possible for service in nuclear-reactor-core components. Two are 1100 series alloys especially useful for structural purposes at low temperatures or for cladding at high temperatures. The third aluminum-base material, a sintered-aluminum product, is considered for both structural and cladding purposes because of its high-temperature strength.

A second aim of this investigation was to observe the cyclic strain-fatigue and creep behavior of aluminum and obtain cyclic stress-strain relations at moderate temperatures for comparison to similar properties to be obtained for higher strength materials suitable for use at high temperatures. Application of data of the type presented here is limited by the analytical methods available. Studies of experimental models of components are sometimes made to provide experimental data on component behavior or confirmation of analytical methods and results. High-purity aluminum might be used for these model studies because its creep properties at reasonable working temperatures allow estimation of the creep behavior of components to be fabricated from high-temperature materials.

Axial cyclic fatigue testing at constant temperatures was utilized in this test program for the following reasons:

1) Preliminary tests and calculations indicated that creep characteristics of aluminum would interfere with determining cyclic plastic strain as a test parameter.

2) Axial fatigue testing facilitates measurement of stress, strain, and time relationships.

3) Constant temperature testing allows evaluation of creep effects.

4) Constant temperature testing may be as realistic as thermal cycling testing since, in actual components, the cyclic thermally induced strain may bear little relation to the direction and amount of temperature change.

Because of the proposed use of aluminum-base material as a fuel element cladding at surface temperatures up to 800°F, it was planned to perform strain-fatigue tests at temperatures ranging between room temperature and 900°F. However, the unstable behavior of 1100-series aluminum alloys at 600°F, evidenced by "necking," yielded results so difficult to interpret that no tests were performed on these materials above 600°F.

II. TEST MACHINE OPERATION

A. GENERAL DESCRIPTION

The basic test machine is a direct, repeated-stress, double unit manufactured by Krouse Testing Machine, Inc. The test machine has a 5000-lb load capacity in tension and compression. Loading beam travel is adjusted by a variable eccentric. The basic machine operates at 1000 cpm. To perform strain-fatigue tests at high temperature, the basic test machine required modifications. Fixtures, special furnaces with controls, temperature monitors, load weighing and recording equipment, and strain measuring equipment were incorporated. These modifications and the method of operation and calibration of the modified machine are described in Reference 1.

B. PLASTIC STRAIN CALIBRATION

The instrumentation described in Reference 1 did not supply information about plastic strain or its relationships to total strain and temperature. A specially instrumented series of tests was performed on the fatigue testing machine to supply calibration of plastic strain vs total strain in the fatigue specimens. To facilitate accurate measurement of strain in the gage length, a 1/8-in.-diameter hole was drilled in each end of the specimen so that the hole bottoms were 0.750 in. apart. Probes were bottomed in the end of each hole and attached to an extensometer. When the specimen was cycled, the extensometer output which was directly proportional to the strain within the 0.750-in. gage length was amplified and recorded by a Model 150 Sanborn continuous recorder coupled with a 1-128 preamplifier. Figure 1 depicts a typical plastic-strain-calibration specimen, and a typical Sanborn deflection record is shown in Figure 2.

The extensometer detected the strain in the 0.750-in. gage length, which includes part of the shoulder radius. Further calibration was required to determine what fraction of this strain occurred in the constant diameter 0.500-in.-long test section. To determine the strain in the test section, wires were attached to the specimen as shown in Figure 1, and an optical micrometer was used to read the movement between tips of the wires. This value was compared with the movement in the 0.750-in. gage length. Effective gage lengths based on these

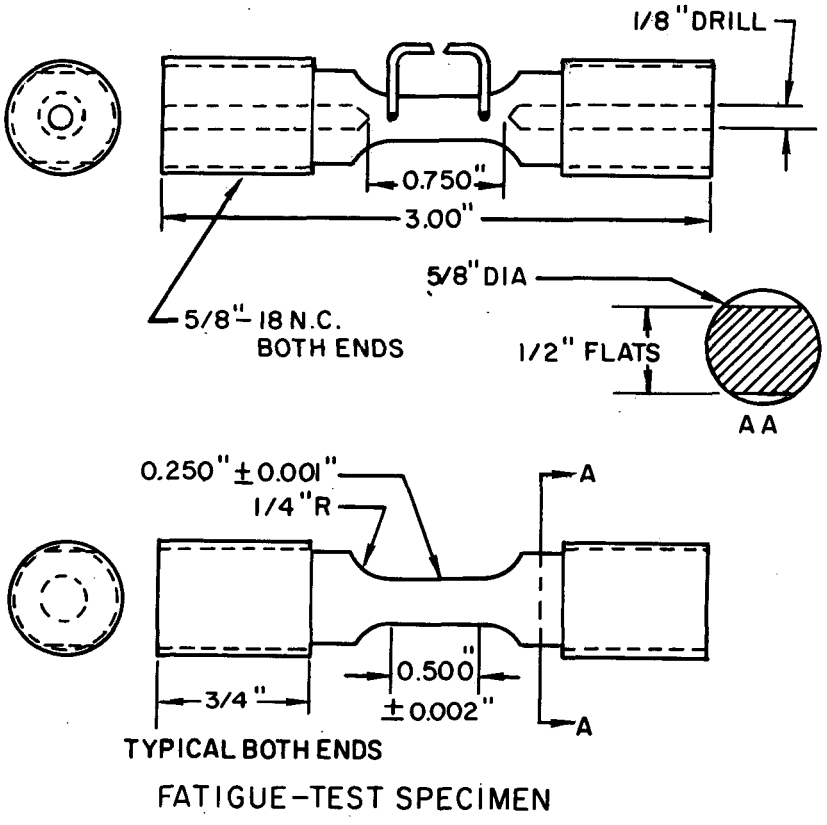

Figure 1. Plastic-Strain-Calibration and Fatigue Test Specimens

measurements, supplemented by a theoretical effective gage length calculated on the basis of elastic behavior, were used in determining actual plastic strain in the 0.500-in.-long test section.

The load on the specimen was detected by a load cell in line with the specimen as described in Reference 1. Output from this load cell was amplified and recorded simultaneously with output from the extensometer on a second channel of the Sanborn recorder. A typical load recording is shown in Figure 2.

The attenuation levels of the recorder for deflection and load channels were calibrated statically before testing, using known deflections and loads to determine mils of deflection and pounds of load per millimeter of chart height.

Plastic strain calibration tests were performed on all three materials at three temperature and six strain levels each.

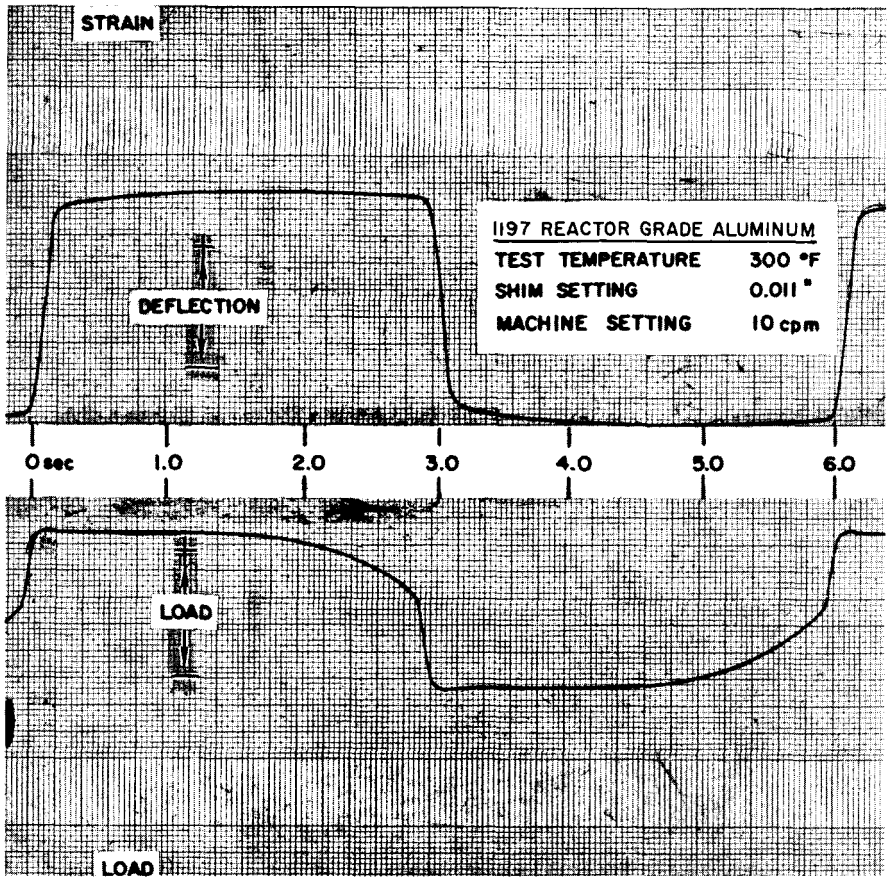

Figure 2. Typical Sanborn Record of Deflection and Load

The stroke of the machine and strain in the specimens is adjusted by insertion of shims in the stroke control fixture. A typical test began at low deflection (0.002-in. shim). Cycling speed of the testing machine was set at 10 cpm, and 3 or 4 cycles were recorded. Shims were increased in steps to 0.013 in., which imparted a total strain of approximately 1.5% to the specimen.

Figures 3 and 4 are plots of stress vs strain for tension and compression cycles of 6-sec duration. Data for these plots came from the Sanborn continuous records using calibration factors to convert chart millimeters to stress and strain. The load zero point was approximated by dividing the total load (σ_T) in half. A line was then drawn at this value, parallel to the x-axis, intersecting the stress-strain curve at two points. The length of the line at zero load between the two intersections indicates the measured plastic strain (ϵ_p). The calculated theoretical plastic strain ($\epsilon_T - \sigma_T/E$) was determined by drawing lines at the slope of the Young's modulus of the material from the points of the largest

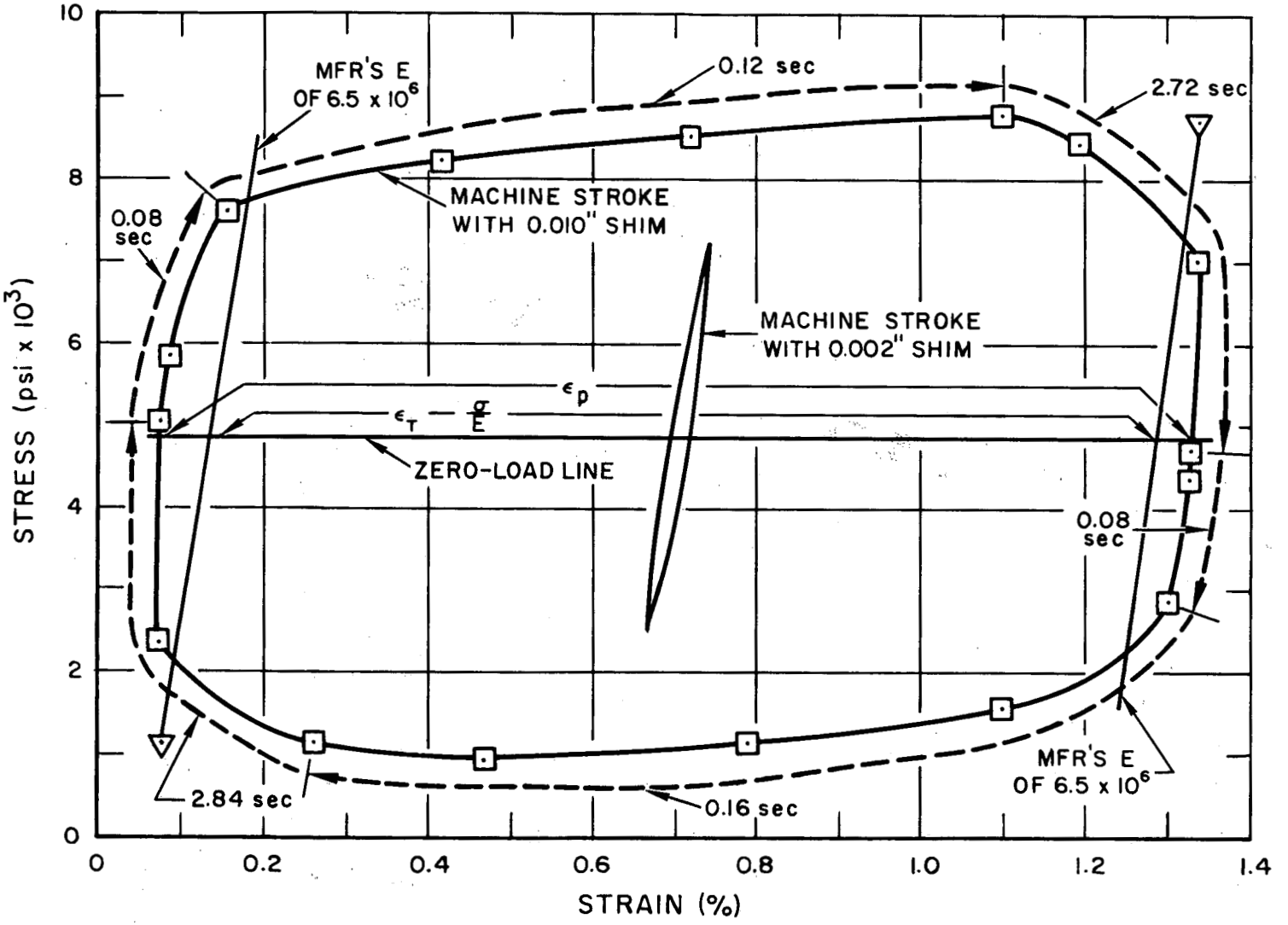

Figure 3. Stress vs Strain Mechanical Hysterisis Loop for 1132 Reactor-Grade Aluminum at 600°F

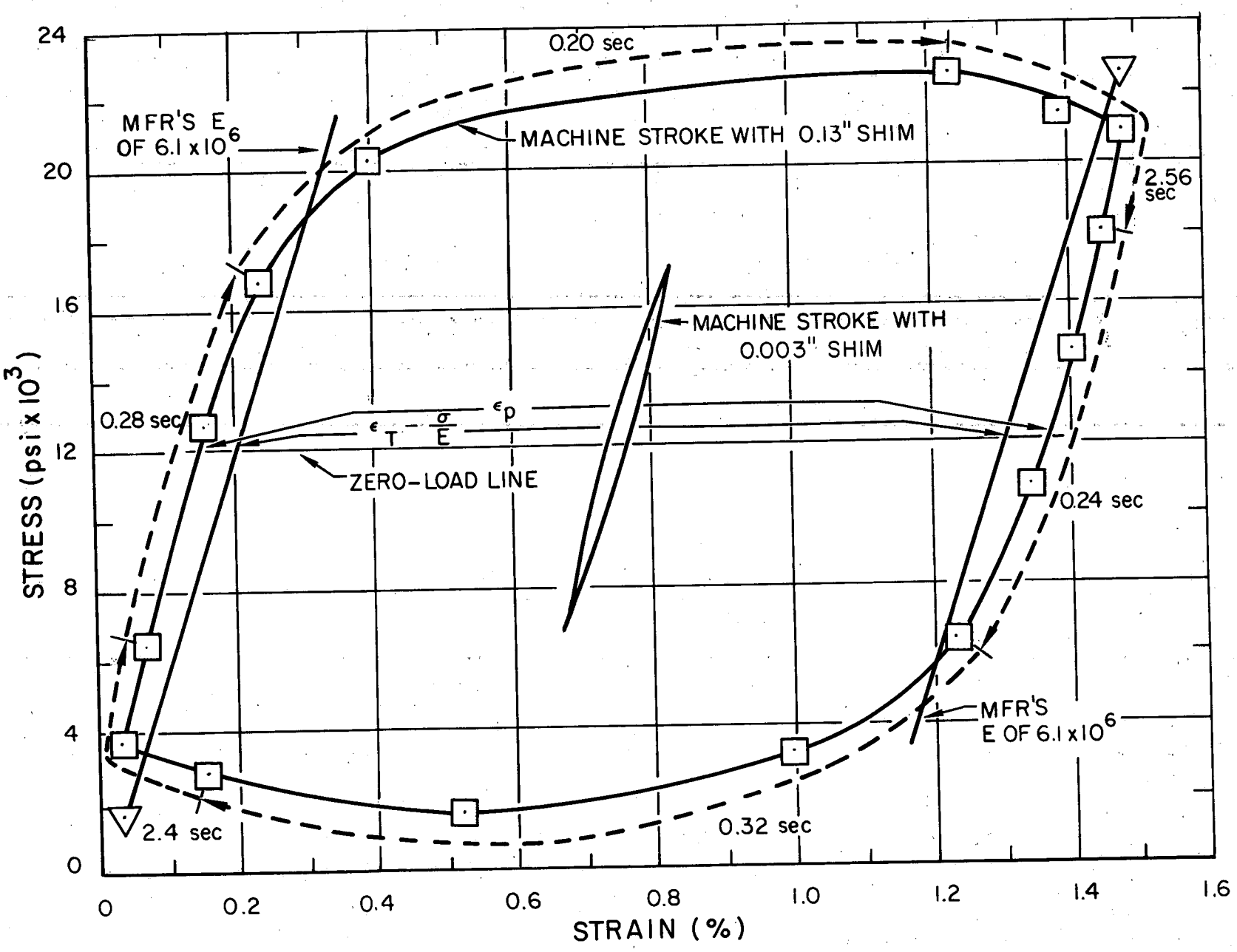

Figure 4. Stress vs Strain Mechanical Hysterisis Loop for Alcoa M-257 at 900°F

negative and the largest positive values of stress and strain. The horizontal distance between these two lines is the calculated theoretical plastic strain ($\epsilon_T - \sigma_T/E$). Both the ϵ_p and ($\epsilon_T - \sigma_T/E$) are defined in Figures 3 and 4. Curves such as Figures 3 and 4 were drawn for each material for each shim value at each test temperature. The values of ϵ_p and ($\epsilon_T - \sigma_T/E$) obtained from these curves were used to plot curves of Figures 5 and 6.

Figure 5 is a plot of plastic strain vs total strain in 1132 alloy at room temperature and 600°F. Figure 6 is a plot of plastic strain vs total strain in Alcoa M-257 (sintered-aluminum product) at room temperature, 600 and 900°F. Data from Figures 5 and 6 are correlated with the fatigue test results in the next section of this report.

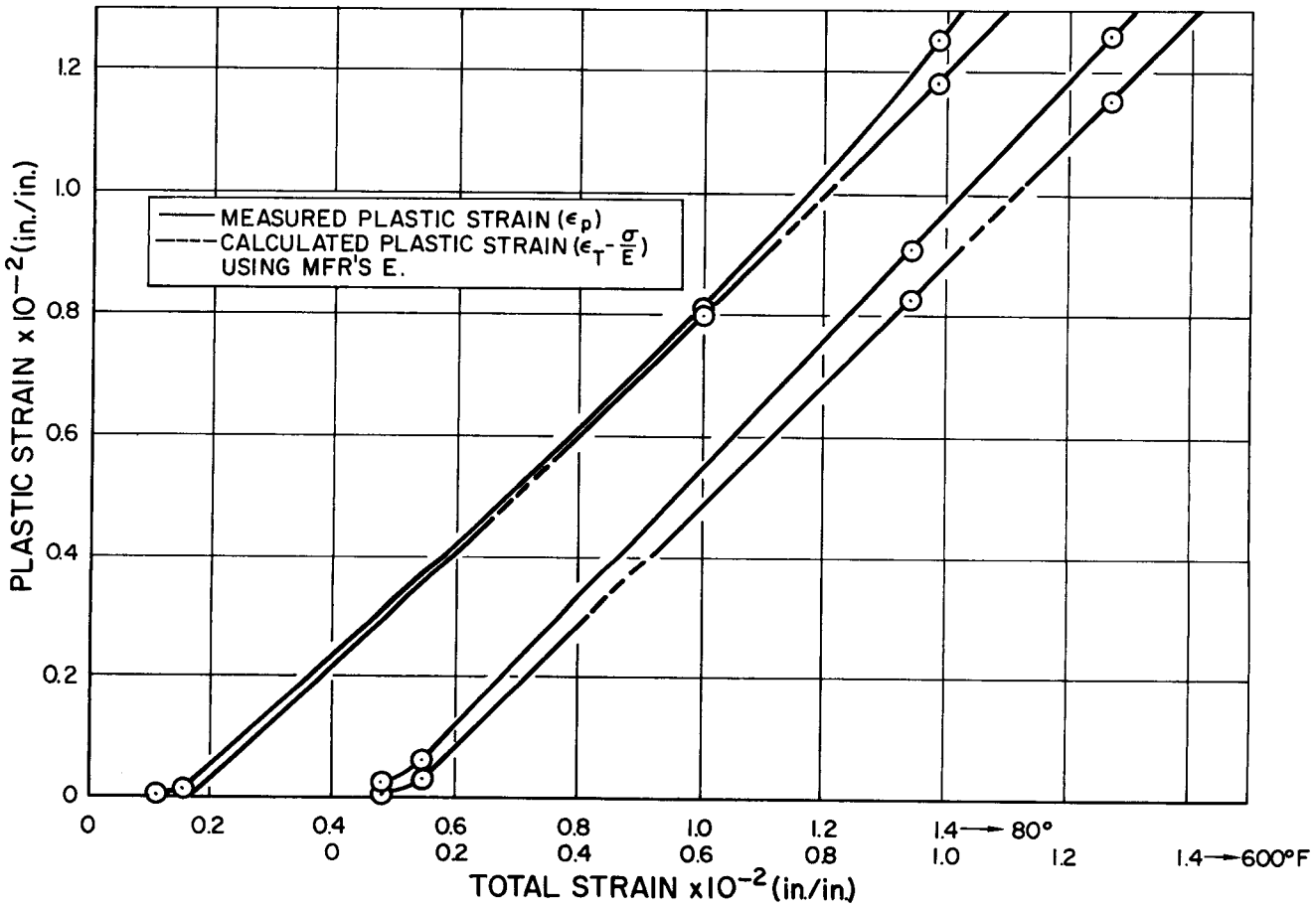

Figure 5. Plastic Strain vs Total Strain for 1132 Reactor Grade Aluminum

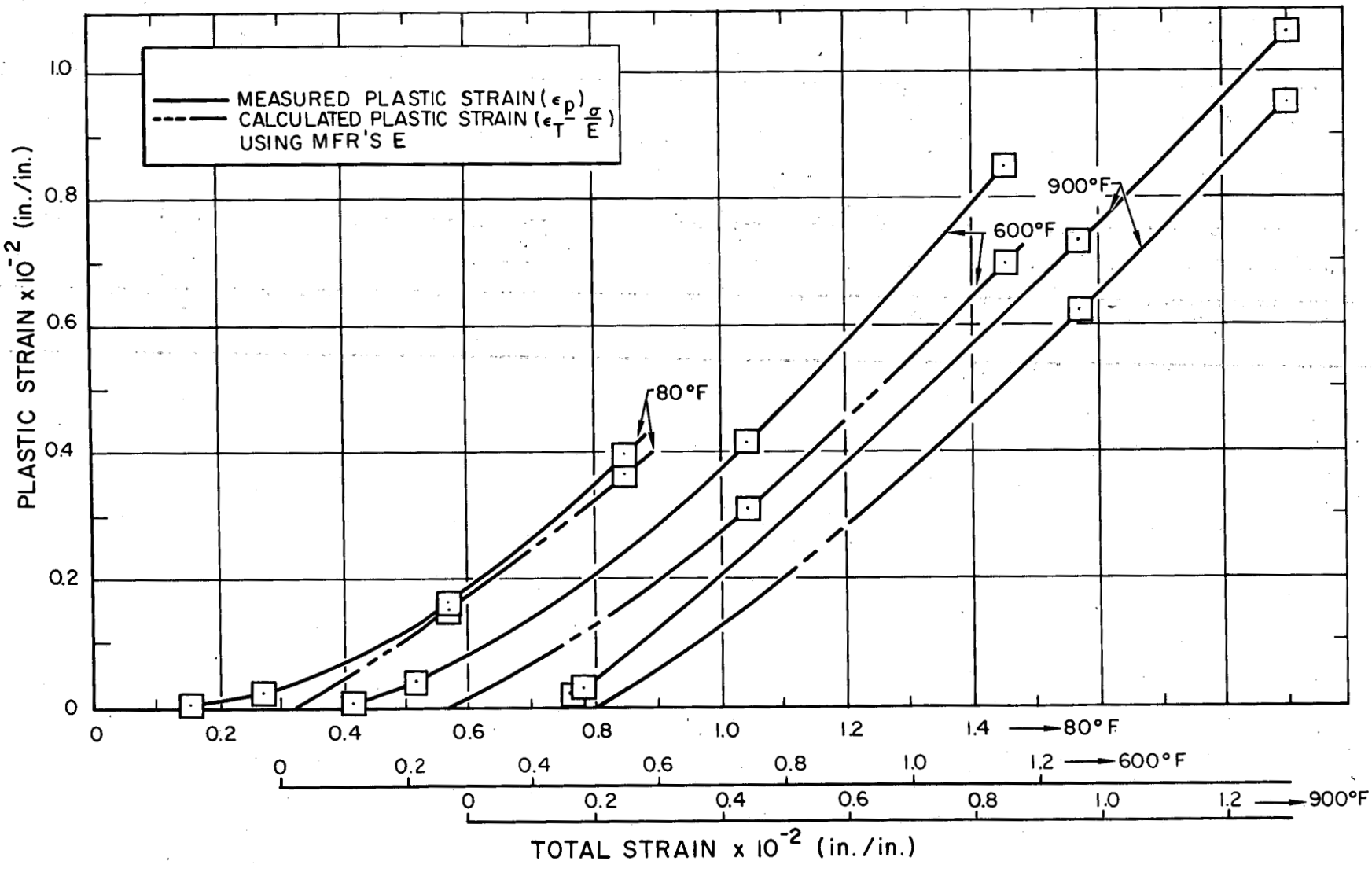

Figure 6. Plastic Strain vs Total Strain for Alcoa M-257

III. TEST RESULTS

A. MATERIAL TESTED

Materials tested in this investigation were 1197 reactor-grade aluminum, 1132 reactor-grade aluminum, and Alcoa M-257 (sintered-aluminum product). The 1197 was received as 1-1/2-in.-thick rolled plate, the 1132 as 1-1/4-in.-diameter extruded bar, and Alcoa M-257 as 5/8-in.-diameter extruded rod. Specimens, as shown in Figure 1, were machined longitudinally to the direction of rolling and extruding.

To obtain cold-worked 1197 alloy, a 1-1/8-in.-diameter bar was machined from the specimen plate stock. This bar was swaged at room temperature from 1-1/8-in. diameter to 5/8-in. diameter. To obtain cold-worked Alcoa M-257, a piece of 5/8-in.-diameter specimen stock was swaged to 1/2-in. diameter. Special adapters were required to use these specimens in the specimen holders.

Chemical analyses of the three materials are presented in Table I. Samples were selected at random from each material. Analyses fell within the expected ranges. A semiquantitative spectrographic analysis was performed on each material. An oxygen analysis was made on M-257 by considering the acid insolubles as Al_2O_3.

Tensile specimens of 1/4-in. gage diameter and 2-in. gage length were machined, from previously mentioned stock, longitudinally to the direction of rolling and extruding for 1197 and 1132 alloys only. These were tested in a universal test machine with a head travel set at 0.05 and 0.35 in./min for determination of physical properties. Measurements were made using a 1-in. gage length.

Tensile specimens of 3/8-in. gage diameter and 2-in. gage length were used in a separate series of tests conducted at Atomics International on extruded Alcoa M-257. The mechanical property data for all three materials are presented in Table II.

TABLE I

CHEMICAL ANALYSES OF SPECIMEN MATERIAL
(Spectrographic Analyses of the Three Lots of Material)

Element	1197	1132	M-257
Al	Remainder	Remainder	Remainder
Fe	0.026	0.44	0.62
Si	0.007	0.17	0.19
Mg	0.005	0.005	0.005
Mn	Nil	0.010	0.009
Ga	Nil	0.012	0.016
Mo	Nil	Nil	0.015
V	Nil	0.030	0.024
Cu	0.001	0.002	0.002
Zn	Nil	Trace	Trace
Ti	Nil	0.007	0.008
Ni	Nil	0.003	0.005
Ca	0.002	0.001	0.004
Cr	Nil	0.002	0.004
Other	Nil	Nil	Nil

Other Analyses:	Carbon in Base Metal	Nil
	Carbon on 1132 fracture surface	0.09% (Lab. 1)
	Carbon in base metal	0.12% Avg (Lab. 1)
	Carbon on 1132 fracture surface	0.17% Avg (Lab. 2)
	Oxygen in M-257 alloy	4.06% as Al_2O_3 (Lab. 2)

B. STRAIN-FATIGUE TEST RESULTS

All strain-fatigue tests were performed at 10 cpm on the modified machine described in the previous section. A continuous recording was made of the number of cycles and load. Twenty type 1197 and twenty type 1132 reactor-grade-aluminum specimens were tested at room temperature, 300 and 600°F. Fourteen Alcoa M-257 specimens were tested at room temperature, 600 and 900°F. The loss of ductility of M-257 during testing resulted in the loss of several specimens during attempted strain calibration tests and depleted the number of specimens

TABLE II

MECHANICAL PROPERTIES OF SPECIMEN MATERIAL

	1197		1132		M-257	
	80°F	600°F	80°F	600°F	80°F	900°F
Yield Point 0.2% Offset (psi x 10^3)	4.35	1.95	11.99	5.01	26.8	7.8
Ultimate Tensile Strength (psi x 10^3)	7.32	2.12	12.91	5.41	36.9	9.1
% Elongation in 4 Diameters	57.2	87.7	26.5	36.5	15.2	5.7
Reduction of Area (%)	~90	~99	~65	~99	33.5	23

available for data. Also, four Alcoa M-257 specimens, which had been cold-worked, were tested at 900°F and six type-1197 cold-worked aluminum specimens were tested at 300 and 600°F. The range of cyclic strain imposed on the specimens was adjusted to obtain a range of cyclic life between 100 and 100,000 cycles. Shape and dimensions of a typical fatigue specimen are shown in Figure 1. Specimens that ran to a very large number of cycles (~2 x 10^5) were taken off test. They are designated by points with attached arrows in figures referenced in this section.

Each specimen test was set to a fixed cyclic strain level by insertion of shims, and the specimen was cycled to failure at that level. The total strain range of the specimens is plotted against the number of cycles to failure in Figures 7, 8, and 9 for the three materials tested.

Figures 10, 11, and 12 present the relation of cyclic stress to cycles to failure for the three materials. Although cyclic strain in the specimens was held fixed throughout each test, the load varied throughout the test. The cyclic load at specimen half-life was taken as the value to obtain the stress values presented. The total stress range represents the total of tension and compression values; consequently, the value of one-half total stress range is presented against cycles to failure representing the customary relationship.

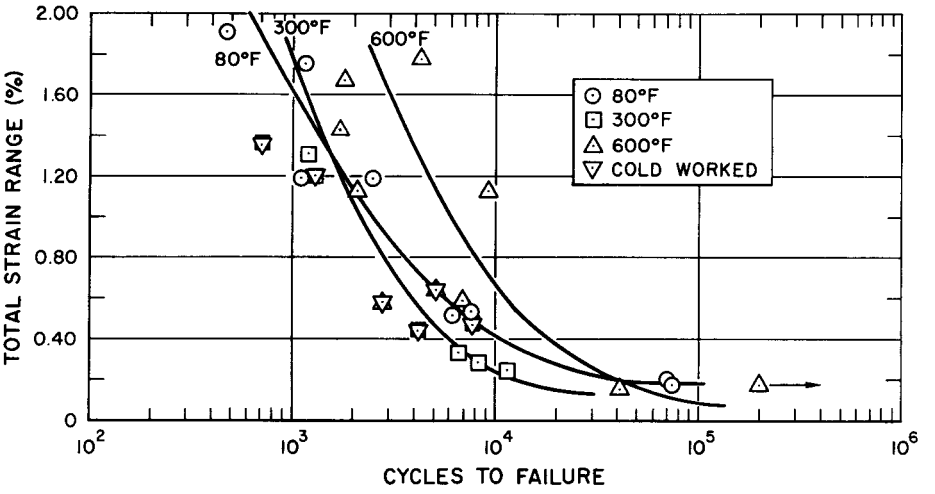

Figure 7. Strain Range vs Cycles to Failure for 1197 Reactor-Grade Aluminum

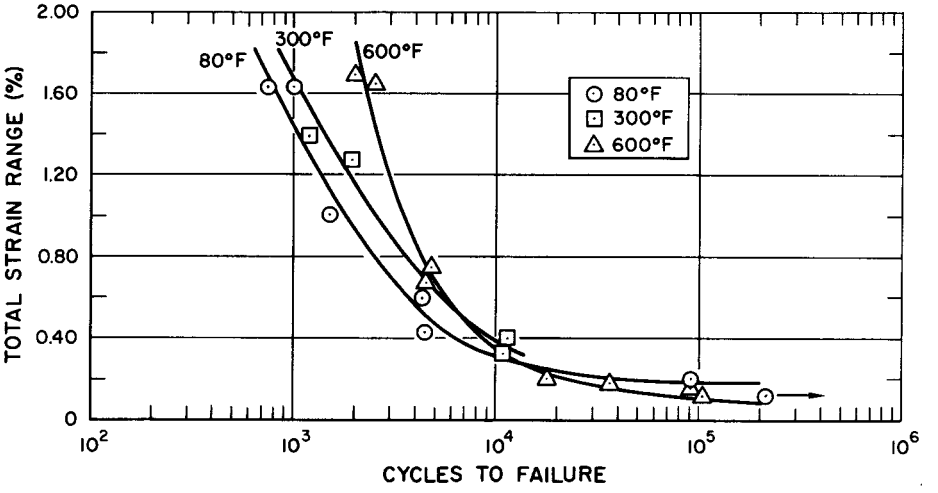

Figure 8. Strain Range vs Cycles to Failure for 1132 Reactor-Grade Aluminum

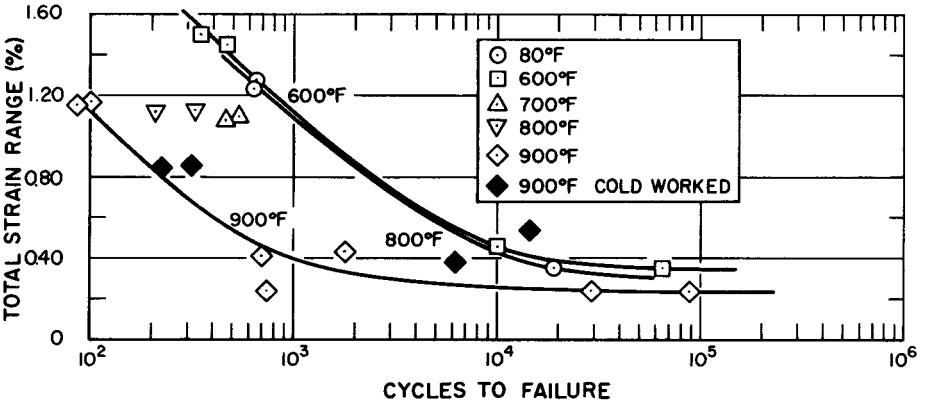

Figure 9. Strain Range vs Cycles to Failure for Aloca M-257

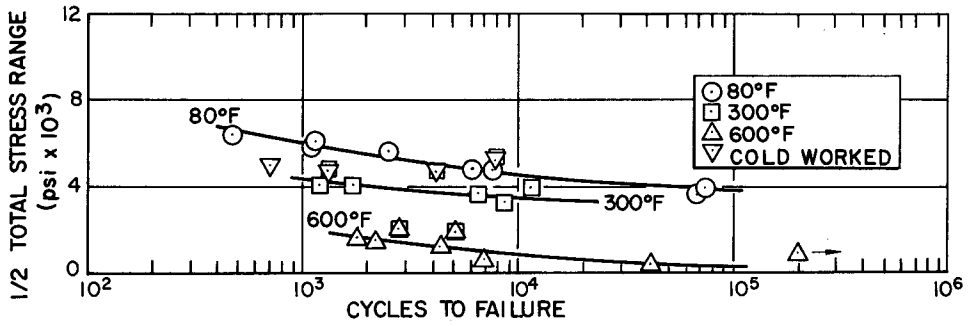

Figure 10. One-half Total Stress Range vs Cycles to Failure for 1197 Reactor-Grade Aluminum

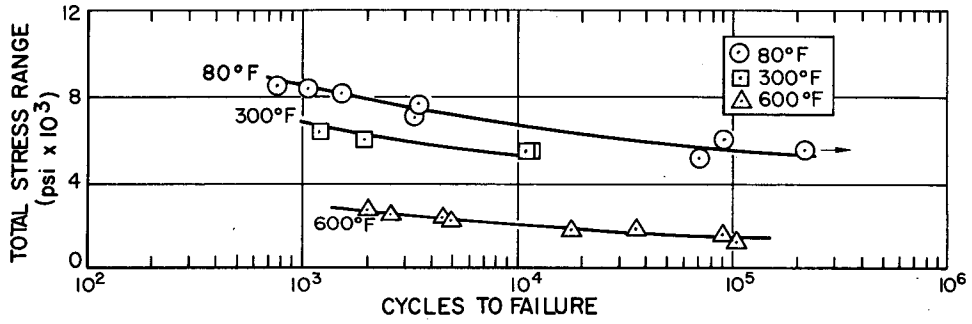

Figure 11. One-half Total Stress Range vs Cycles to Failure for 1132 Reactor-Grade Aluminum

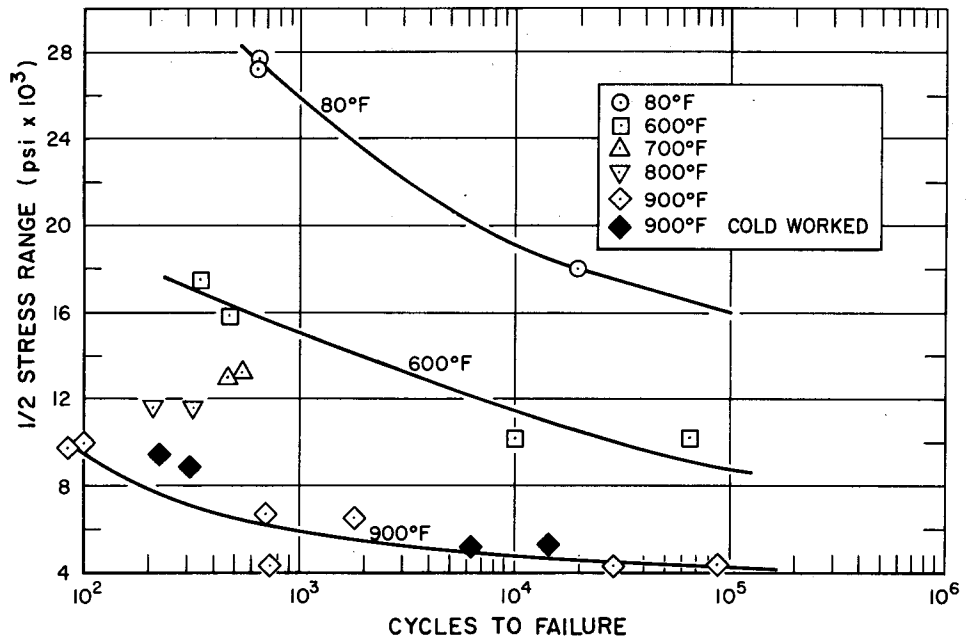

Figure 12. One-half Total Stress Range vs Cycles to Failure for Aloca M-257

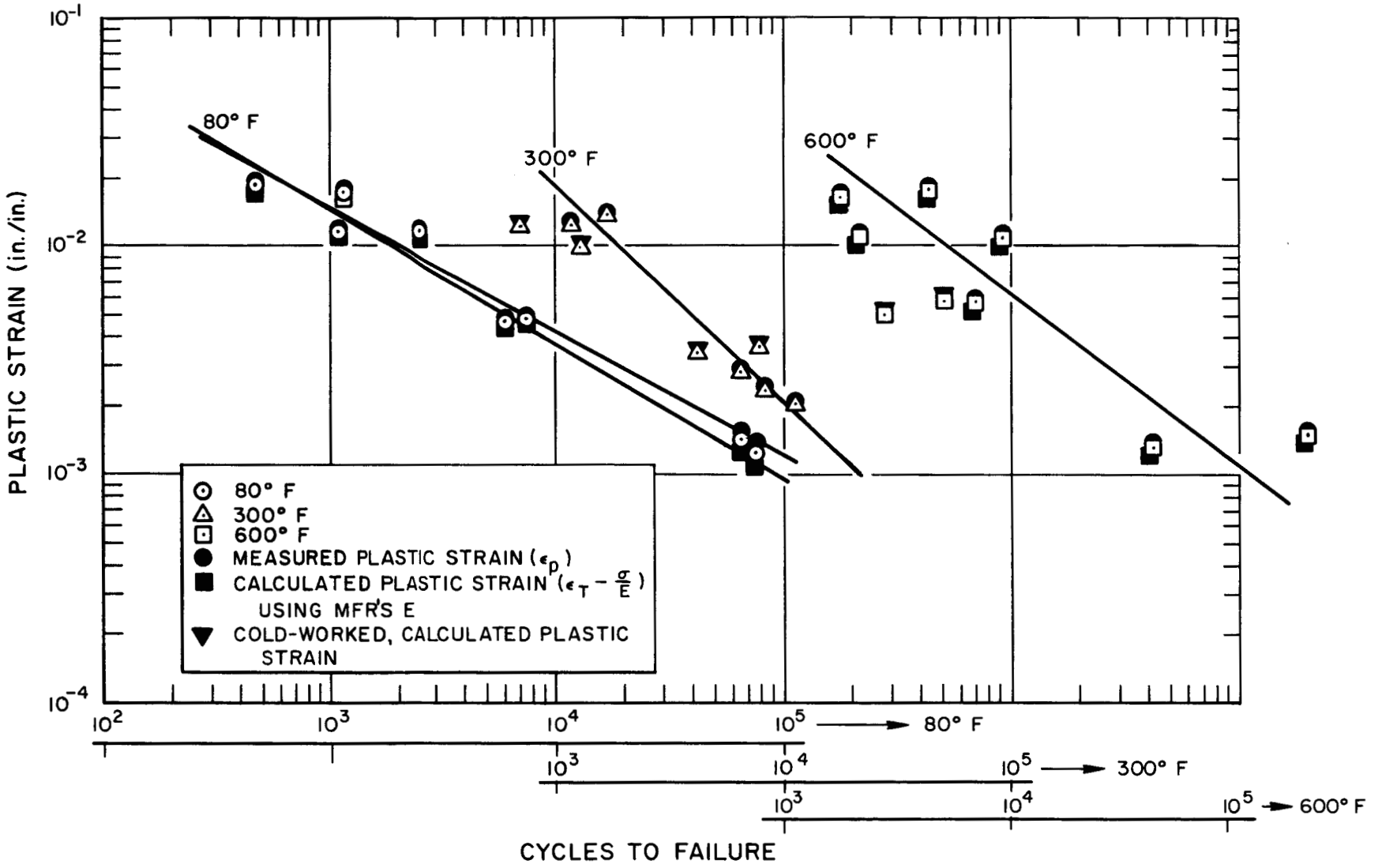

Figure 13. Plastic Strain vs Cycles to Failure for 1197 Reactor-Grade Aluminum

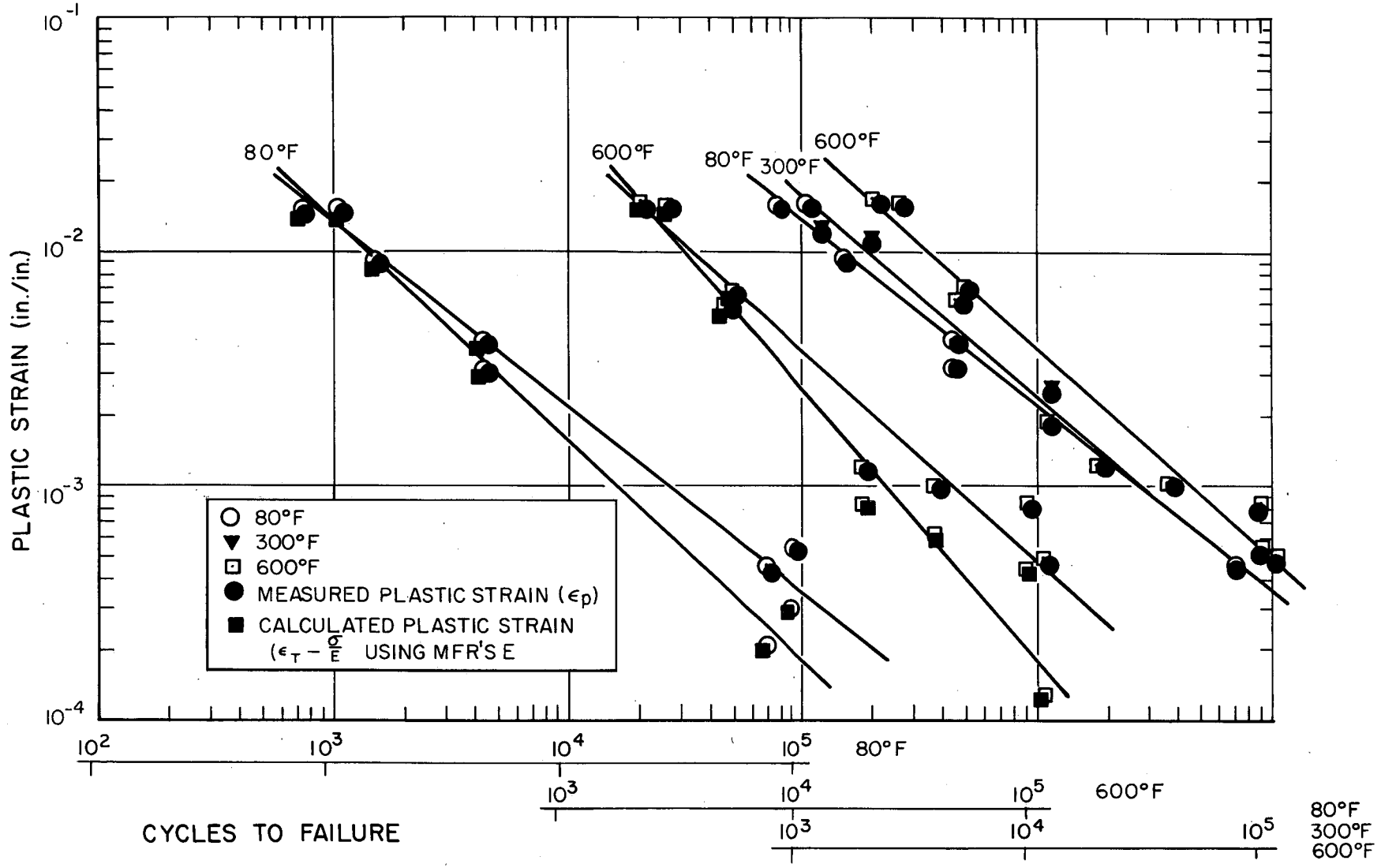

Figure 14. Plastic Strain vs Cycles to Failure for 1132 Reactor-Grade Aluminum

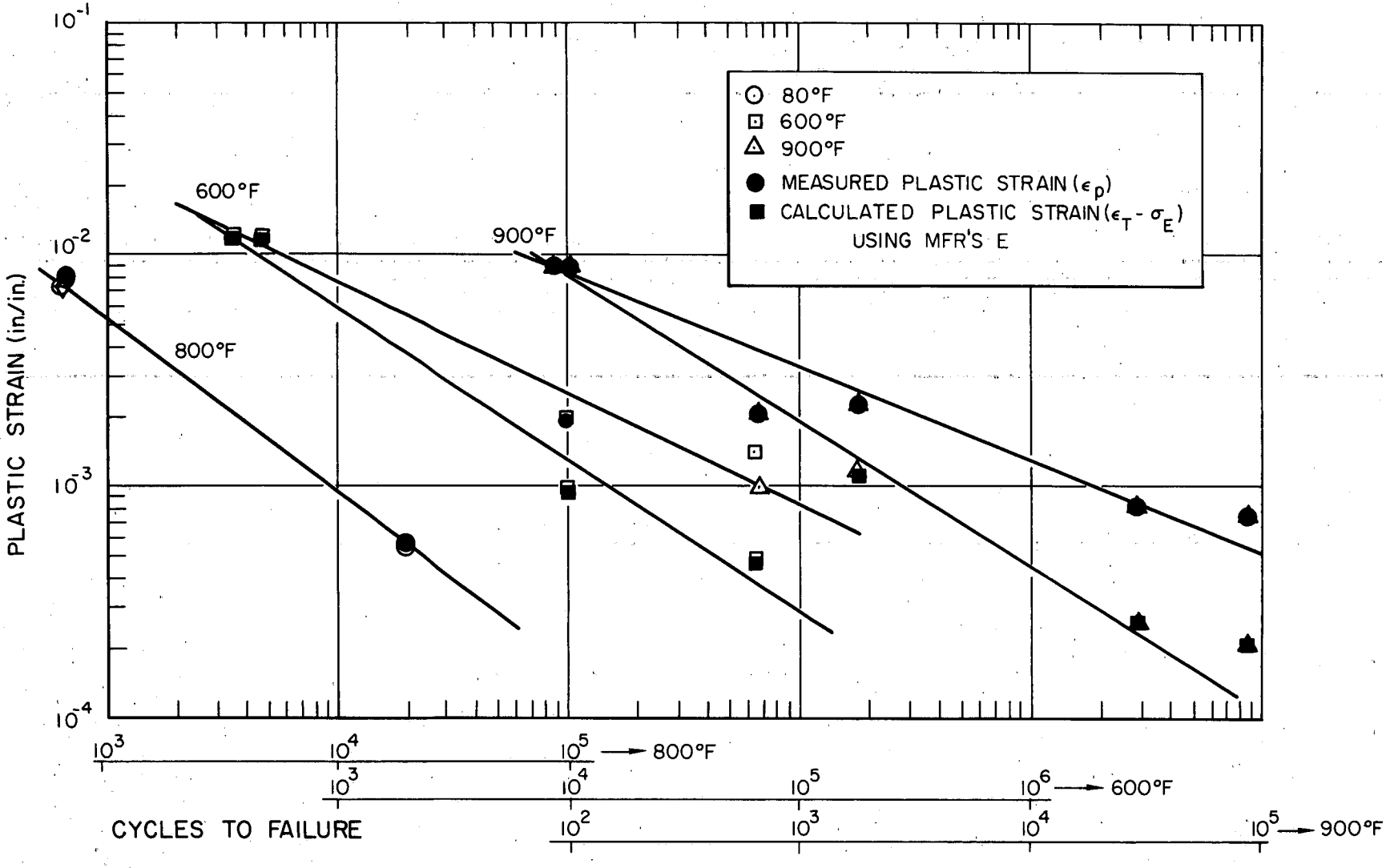

Figure 15. Plastic Strain vs Cycles to Failure for Alcoa M-257

Another set of curves was drawn by utilizing the plastic strain vs total strain calibration presented in Section I-B, and the total strain vs cycles to failure relationships from the tests. The results of this cross plot, plastic strain vs cycles to failure, are shown in Figures 13, 14, and 15. Each figure encompasses three test temperatures and includes curves of both measured and calculated theoretical plastic strain.

The Alcoa M-257 data at room temperature and 600°F appeared characteristic of ductile materials. Because there was a gap in the behavioral picture between 600 and 900°F, four specimens that were to be tested at room temperature were tested at 700 and 800°F (two at each temperature). The data obtained were used in preparing Figure 16. The curve presents the number of cycles to failure at 0.75% plastic strain vs test temperature. Also, in Figure 16 is a curve of percent elongation in four diameters vs test temperature. Data for this curve were obtained from Reference 3.

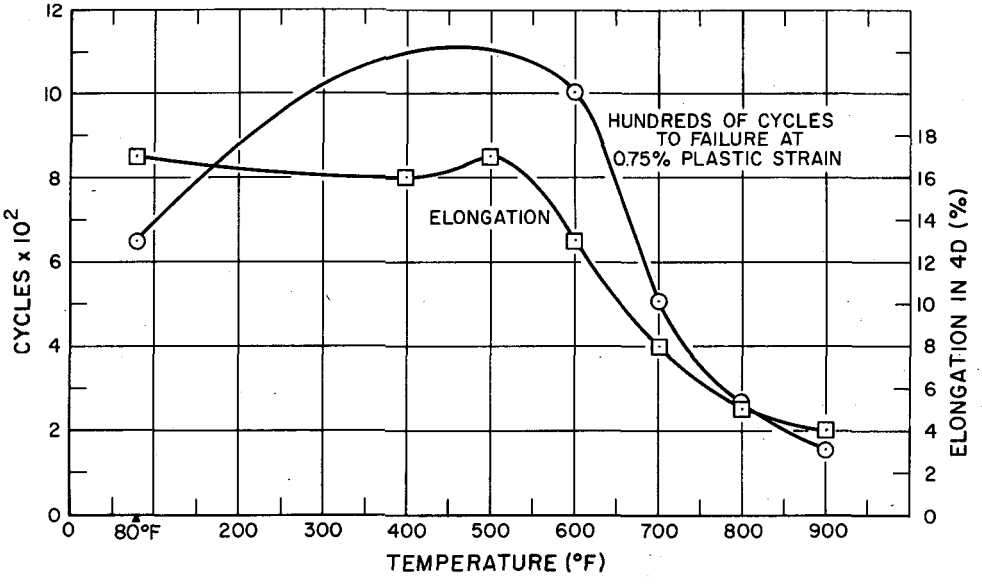

Figure 16. Cycles to Failure and Elongation vs Test Temperature for Alcoa M-257

C. RESULTS OF METALLOGRAPHIC EXAMINATION

A number of samples were chosen from each of the three materials for macroscopic and microscopic examination. From each material, samples were chosen to represent results of testing at high and low strains and at high and low

temperatures. All samples were sectioned longitudinally, polished, and etched. They were found to be sound and uniform except for defects caused by fatigue testing. Photographs of typical samples are shown in Figures 17, 19, and 24. The samples for microscopic examination were mounted and etched. The microstructure of Alcoa M-257 could not be defined with any of several etching techniques tried. The 1197 and 1132 aluminum microstructures were defined satisfactorily with conventional techniques. Typical microstructures were photographed and are shown in Figures 21, 22, 23, 26, 27, 28 and 29.

After fatigue failure occurred on all three types of specimens, black deposits were noticed on some of the fracture surfaces. The size and orientation of these deposits obviate the possibility that they were inherent in the specimen material.

These deposits were examined by x-ray diffraction and found to be non-crystalline. Subsequent analyses by conventional methods showed that the deposits were carbonaceous. Since the deposits appeared only on the fracture surface, it is believed that they were deposited during or after testing from decomposition products of lubricants used in the machine specimen holders. Figure 25 shows a typical black deposit on a fracture surface.

The "necking" of 1197 and 1132 aluminum specimens occurred at room temperature, 300, and 600°F. Magnitude of the deformation increased with the total strain setting for each test as can be seen in the photographs. Identification, test data, and specific comments for each specimen shown are listed underneath the photographs.

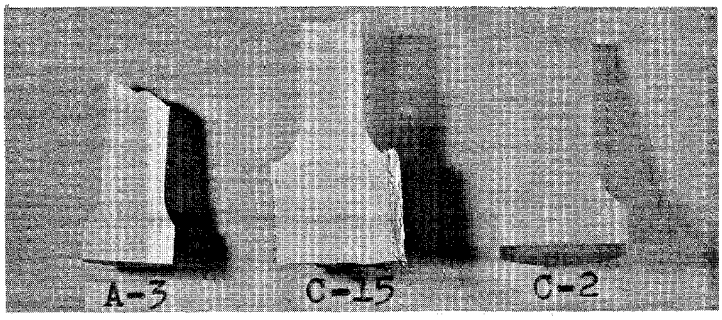

Figure 17. Structure of Alcoa M-257 Samples [From left to right: Specimens CW-4 (cold-worked material tested at 1.03% strain at 900°F... failed at 225 cycles); 2M7 (tested at 0.24% strain at 900°F... failed at 87,500 cycles); and 1M3 (tested at 0.31% at room temperature... failed at 22,050 cycles). Samples show structure typical of the M-257 alloy. Samples were sound and uniform. No gross deformation or extensive surface cracking was observed on the specimens.] (1X)

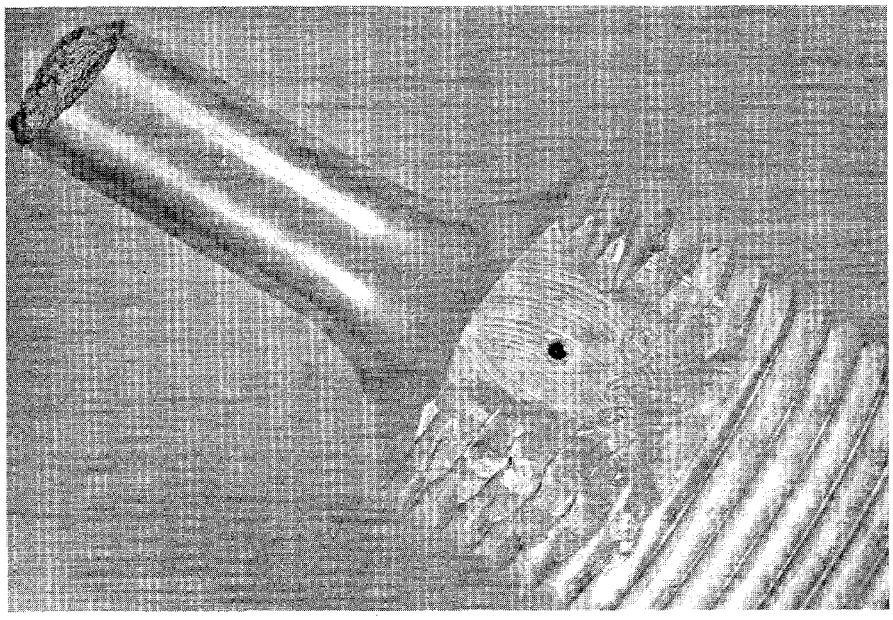

Figure 18. Fracture of Alcoa M-257 Sample [Specimen 2M9 (tested at 0.43% strain at 900°F... failed at 1800 cycles). Specimen shows a fracture typical in the M-257 material] (~4X)

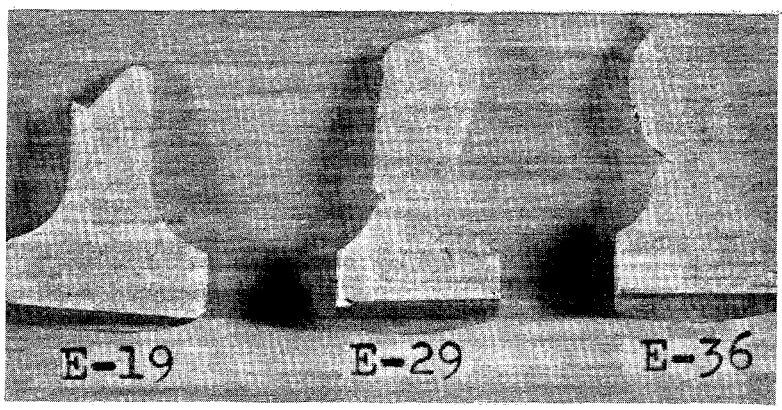

Figure 19. Structure of Three Samples of 1132 Reactor Grade-Aluminum [From left to right: Specimen II-4 (tested at 0.19% strain at room temperature... failed at 69,450 cycles); II-13 (tested at 0.12% strain at 600°F ... failed at 106,350 cycles); II-16 (tested at 1.69% strain at 600°F... failed at 2000 cycles). Samples show the changes in structure that occurred during testing.] (~2X)

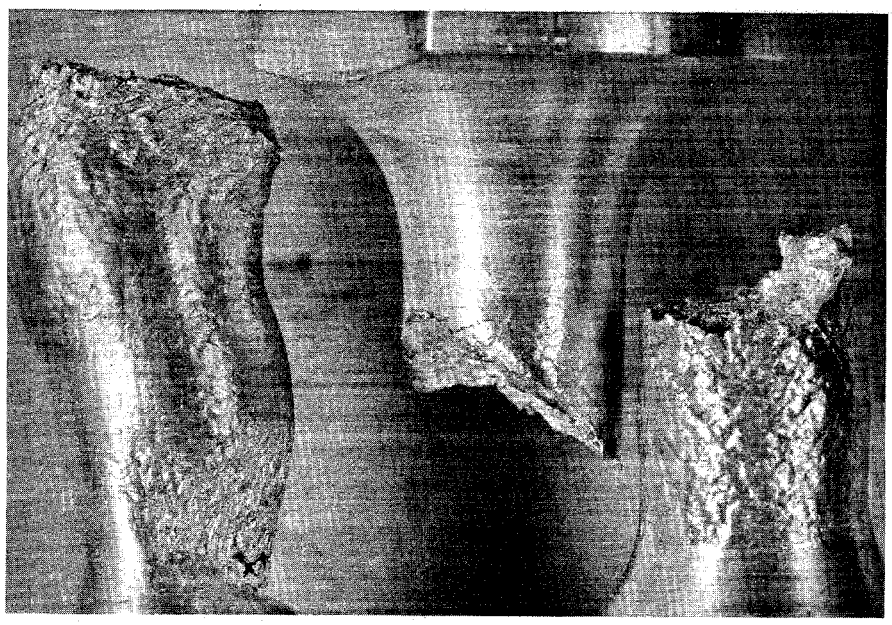

Figure 20. Fracture of Three Samples of 1132 Reactor-Grade-Aluminum [From left to right: Specimens II-8 (tested at 0.18% strain at 600°F... failed at 36,650 cycles); II-6 (tested at 0.20% strain at room temperature... failed at 90,850 cycles); II-11 (tested at 1.63% strain at room temperature...failed at 1030 cycles). Failures occurred after material "necked" at shoulder of specimen (left), in a normal manner (center), or after extensive surface cracking (right).] (~4X)

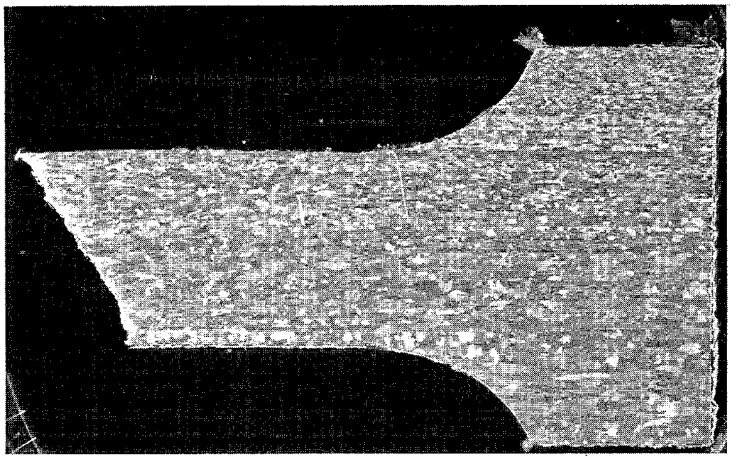

Figure 21. Microstructure of 1132 Sample Fatigued at Room Temperature [Sample Specimen II-6 (tested at 0.20% strain at room temperature... failed at 90,850 cycles). Structure was unaltered. Fracture appears to be typical of fatigue failure.] (~4K)

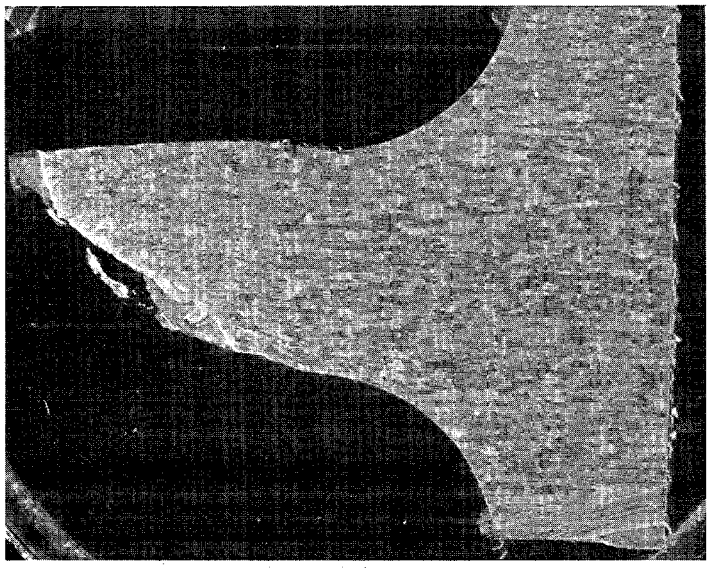

Figure 22. Microstructure of 1132 Sample Fatigued at 300°F [(Specimen II-2 (tested at 0.40% strain at 300°F... failed at 11,400 cycles). Unworked shoulder of the specimen appears unaffected by temperature. Worked portion in the gage length shows considerable grain refinement and reorientation. Some surface roughening occurred. Fracture is in maximum shear direction.] (~4X)

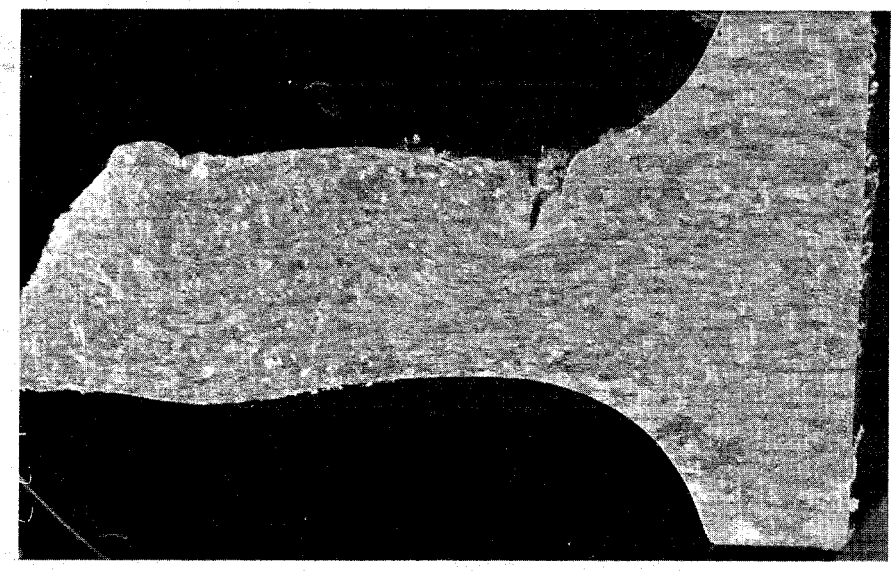

Figure 23. Microstructure of 1132 Sample Fatigued at 600°F [Specimen II-15 (tested at 0.16% strain at 600°F... failed at 91,000 cycles). No significant change in grain size is apparent; however, the effects of working are obvious.] (~4X)

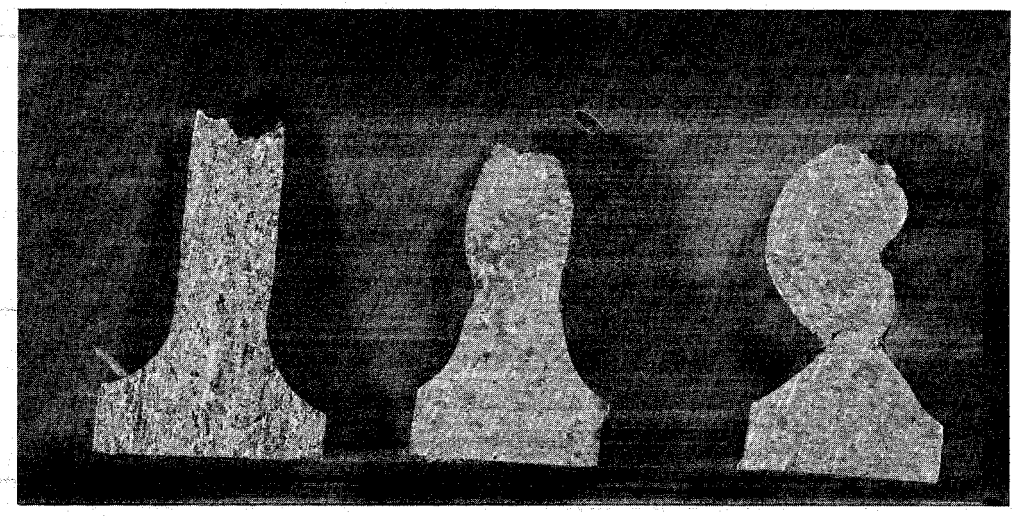

Figure 24. Structure of Three Samples of 1197 Reactor-Grade Aluminum [From left to right: Specimens III-A6 (tested at 0.20% strain at room temperature... failed at 66,900 cycles); III-A22 (tested at 0.16% strain at 600°F... failed at 41,150 cycles); and III-A13 (tested at 1.78% strain at 600°F... failed at 4300 cycles).] (~3X)

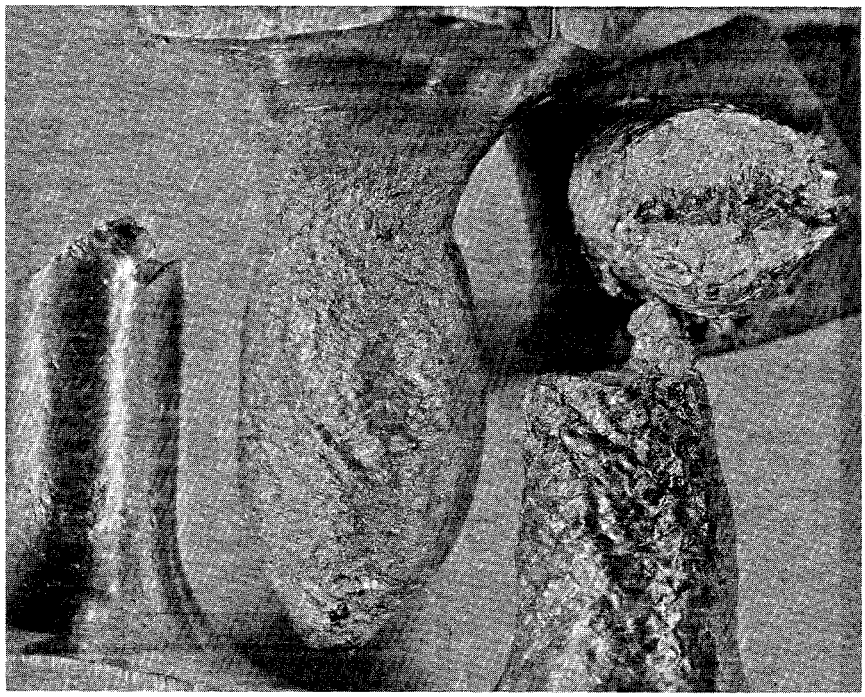

Figure 25. Fracture of Four Samples of 1197 Reactor-Grade Aluminum [From left to right: Specimen III-A2 (tested at 0.18% strain at room temperature... failed at 74,150 cycles); III-B5 (tested at 0.25% strain at 300°F...failed at 11,500 cycles); III-B2 (tested at 1.44% strain at 300°F... failed at 1700 cycles); and III-A11 (tested at 1.67% strain at 600°F... failed at 1800 cycles). Samples show types of fracture that occurred in alloy; "necking" seem to be function of total strain and temperature. Specimen III-B2 shows network of five cracks that occurs mainly in maximum-shear direction and seems insensitive to grain boundaries. Specimen III-A11 shows black deposit that occurred on many of the fracture surfaces.] (~4X)

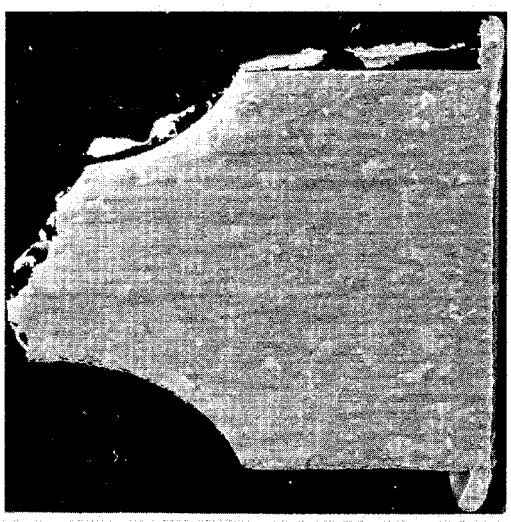

Figure 26. Microstructure of 1197 Sample Fatigued at Room Temperature [Specimen III-A6 (tested at 0.20% strain at room temperature... failed at 66,900 cycles). Little or no change in grain size or orientation.] (~4X)

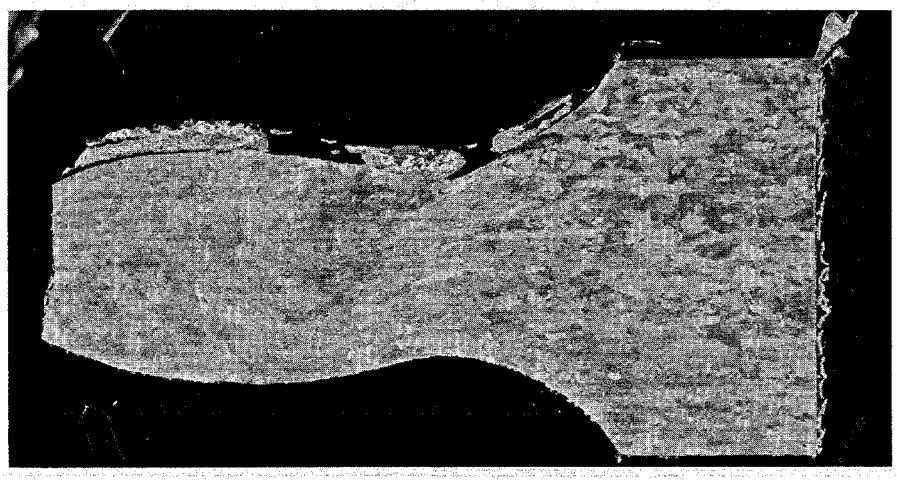

Figure 27. Microstructure of 1197 Sample Fatigued at Room Temperature [Specimen III-A8 (tested at 1.91% strain at room temperature... failed at 470 cycles); "necking" occurred at shoulder of specimen. Grain size of worked portion was reduced, and its orientation was changed.] (~4X)

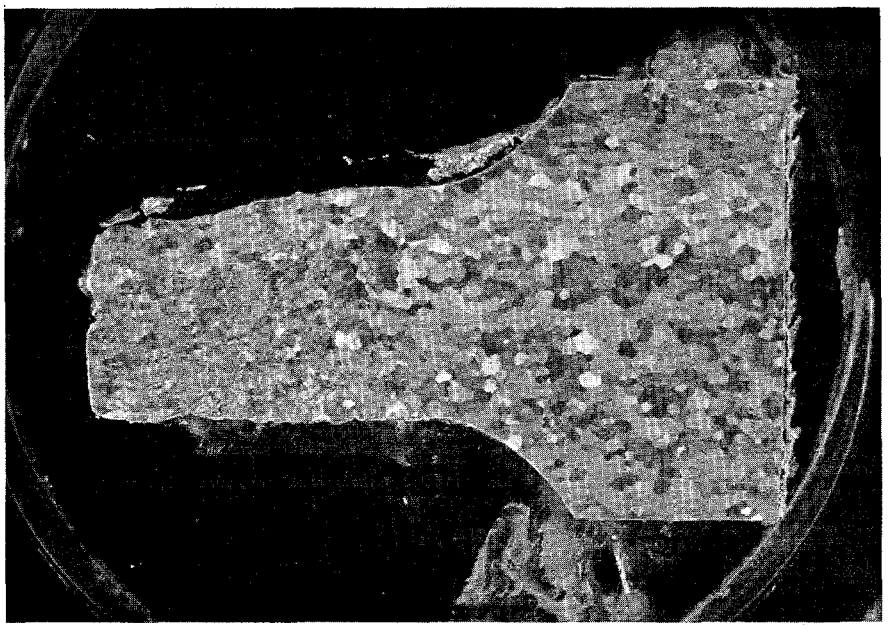

Figure 28. Microstructure of 1197 Sample Fatigued at 300°F [(Specimen III-B3 (tested at 1.31% strain at 300°F... failed at 1200 cycles). Extensive recrystallization has occurred, and the original structure has entirely disappeared.] (~4X)

Figure 29. Microstructure of 1197 Sample Fatigued at 600°F [Specimen III-A13 (tested at 1.78% strain at 600°F... failed at 4300 cycles). A good example of "necking" of specimen in 0.250-in.-original-diameter section is shown here. Grain size has been reduced markedly in the portions where working was concentrated. Fracture finally occurred in one of these fine-grained sections. Material in background is mounting putty.] (~4X)

IV. DISCUSSION OF RESULTS

A. TEMPERATURE, DUCTILITY AND CYCLIC-LIFE RELATIONS

1. Effect of Temperature on Ductility

Results of tensile tests listed in Table II indicate a significant increase in ductility with increase in temperature for the 1100-series aluminum alloys. This increase in ductility is apparent in the data on both elongation and reduction of area. Elongation at fracture increases 35 to 50% with a rise in test temperature from 80 to 600°F. Reduction of area at the fracture surface was so great at 600°F that precise measurement was impossible.

The Alcoa M-257 results indicate a loss of ductility with increase in temperature apparent in both elongation and reduction of area. Figure 16 presents additional data on variation in elongation with specimen test temperature from Reference 3.

2. Relation of Ductility to Cyclic Life

Figures 7 and 8 indicate that for equal values of cyclic strain, there tends to be an increase in cyclic life with temperature for both 1100-series aluminum alloys. At high strain ranges this appears as a factor of three on cycles between 80 and 600°F. At lower cyclic-strain levels this ratio is reduced so that on a total strain basis, the 80°F cyclic life is greater than the 600°F life, while on a plastic-strain basis little difference appears between the cyclic life at 80 and 600°F.

The effect of the unstable specimen behavior resulting in "necking" at high test temperatures and high values of cyclic strain introduces significant error in the cyclic-strain values noted for these tests. Examination of the "necked" areas of the specimens leads to estimates of strain five times as high as the recorded average value over the gage length. Since this "necking" occurred principally in the high temperature tests, the results are conservative and it appears that the effect of temperature and ductility would be to yield a much greater increase in cyclic life with increase in temperature than that indicated in the test results.

Figure 16 demonstrates the relation between ductility, as measured by elongation in 4 diameters, and cyclic life for Alcoa M-257. The difference in cyclic life is based on equal values of cyclic plastic strain and would be even greater if based on equal values of total cyclic strain.

All alloys showed a significant decrease in cyclic life for equal values of cyclic stress range as the test temperature was increased.

The cold-worked specimens were tested primarily to detect any variation in the unstable characteristics or in the metallurgical behavior of the specimen. No significant change in these characteristics was detected. Results of the tests did indicate a decrease in cyclic life for equal values of cyclic strain for the 1100-series and an increase in cyclic life for the M-257 alloys when the material had been cold worked.

B. INTERPRETATION OF PLASTIC STRAIN

Observations of cyclic strain with a telescopic micrometer were made during the initial high-temperature tests on the fatigue machine. These observations indicated that creep strain was occurring in the specimens during the period when the movement of the machine was halted by the mechanical stops. Such movement could affect the estimation of plastic strain occurring in a test by allowing additional elongation of a fatigue specimen while the load on the specimen was being relaxed. This would negate the expression used to calculate plastic strain, $\epsilon_p = \epsilon_T - \sigma_T/E$, since peak stress and peak strain would not occur simultaneously. Figures 3 and 4 show that there is a significant increase in strain while the load is decreasing and indicate the difference between calculated and measured plastic strain. Figures 5 and 6 show the magnitude of error in plastic strain estimation existing over a range of strain when plastic strain is estimated by the expression, $\epsilon_p = \epsilon_T - \sigma_T/E$.

Data of Figures 13, 14, and 15 may be represented by a straight line on log-log paper. This indicates compliance with the fatigue law $N^k = C\epsilon_p$ as proposed by Manson,[4] where N = number of cycles to failure, ϵ_p = plastic strain and k and C are experimentally determined constants. This straight line relationship on log-log paper appears to hold true whether considering calculated or measured plastic strain. Table III presents the value of the constants k and C determined from these figures for both calculated and measured plastic strain.

TABLE III

CONSTANTS "k" and "C" FOR FORMULA $N^k = C\epsilon_p$

Material	Test Temperature (°F)	Calculated Plastic Strain		Measured Plastic Strain	
		k	C	k	C
Aluminum Alloy 1197	80	-0.60	1.04	-0.55	1.54
	600	-0.76	0.145	-	-
Aluminum Alloy 1132	80	-0.945	0.1075	-0.80	0.294
	600	-1.16	0.00877	-0.90	0.065
Sintered-Aluminum Product Alcoa M-257	80	0.75	1.05	-	-
	600	0.65	1.92	0.48	4.69
	900	0.63	6.85	0.40	18.9

In all cases the value of k has a lower value on the basis of measured plastic strain than on the basis of calculated plastic strain.

The magnitude of creep strain which could occur during the hold period of one-half a strain cycle is expressed as:*

$$\epsilon_C = t \cdot B\sigma_{yp}^{\ n}\left[1 - \frac{tn}{2}\frac{kL}{\sigma_{yp}A}B\sigma_{yp}^{\ n}\right] .$$

Examination of this expression indicates that the magnitude of this creep strain is primarily proportional to the creep rate constant B, the hold time t at the end of the stroke, and to some power n of the stress range during the test. The second term in the parentheses shows that the creep-strain rate decreases by a factor proportional to the ratio of machine stiffness K (spring rate) to specimen strength (area A times yield strength σ_{yp}). The significance of this ratio may be interpreted as follows:

1) A specimen of greater yield-strength material or greater cross section would induce greater elastic deformation of the test machine and allow more creep strain to be imposed on the specimen during the hold time.

*See Appendix for derivation.

2) A more elastic machine, lower value of K, would also result in greater elastic deformation of the test machine and increased creep strain.

This term also indicates that a longer specimen with a larger ratio of specimen strain to machine strain would be less sensitive to creep-strain error.

These observations are substantiated by the results of the strain calibration tests shown on Figures 3 and 4. Since creep rates increase exponentially with temperature, there is an increase in error in plastic-strain estimate with temperature despite a decrease in yield strength by a factor of 3 or 4. Alcoa M-257 has a yield strength at 900°F almost as high as that of 1132 alloy at 80°F and higher than that of 1197 alloy. Also, Alcoa M-257 shows a larger error in estimate of plastic strain at 900°F than the 1100-series alloys show at 80°F. The result of the error in calculating plastic strain is to underestimate the amount of cyclic plastic strain which will result in failure at a given number of cycles. This leads to presentation of data in a conservative form.

V. CONCLUSIONS

1) The test technique described in this report is not satisfactory for obtaining accurate strain-fatigue data for highly ductile materials because of instability "necking" of the specimens. However, data obtained are conservative. This same instability may affect its usefulness for model studies.

2) Data presented herein are usable in the analytical design of components subjected to thermal-strain cycling. Because of the behavior of the materials at higher temperatures, tests on prototypes may be required to substantiate predicted performance at these temperatures.

3) The rapid loss of ductility in Alcoa M-257 at temperatures above 600°F requires special consideration in design of components, and merits further investigation.

4) There is a close correlation between ductility and strain-fatigue life for the three materials tested.

5) Plastic strain is not accurately expressed by $\epsilon_p = \epsilon_T - \sigma_T/E$ when the material is being tested under conditions where creep or load relaxation can occur. The elastic characteristics of the test machine affect the amount of error imposed.

6) Calculation of cyclic plastic strain data on the basis of $\epsilon_p = \epsilon_T - \sigma_T/E$ leads to presentation of data in a conservative form.

7) Results of strain fatigue tests on aluminum based materials may be expressed by the plastic strain fatigue law $N^k = C\epsilon_p$. The values of k and C for each material varies with temperature. Values of k and C determined from calculated plastic strain do not agree with those determined on the basis of measured plastic strain.

APPENDIX

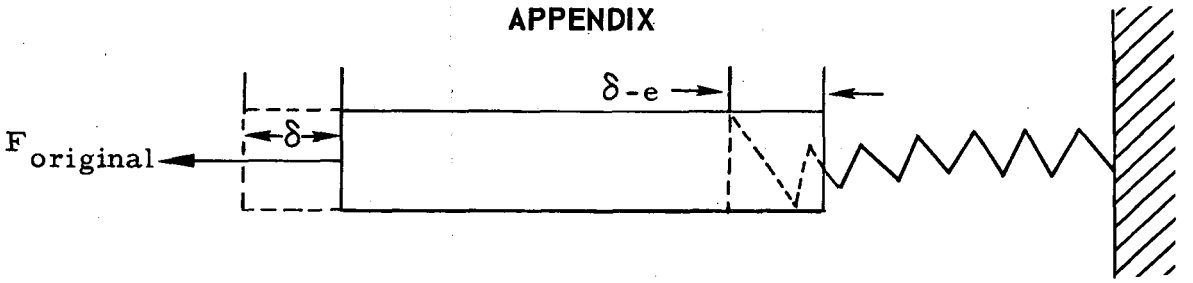

Let:

δ = deflection of left end of specimen from prosition (1) to (2) due to force, held constant during time interval t,

e = change in physical length of specimen due to creep strain and initial elastic and plastic strain represented by e_c, e_E and e_p respectively,

$e = e_E + e_p + e_c$,

K = spring constant, whose value depends on the elasticity of the test machine.

The original force on the rod is,

$$F_{original} = K\left[\delta - e\right] = K\left[\delta - (e_E + e_p)\right] .$$

The resultant force on the rod after creep strain occurs is,

$$F_{resultant} = K\left[\delta - e\right] = K\left[\delta - (e_E + e_p + e_c)\right] .$$

Therefore, the change in the magnitude of the force acting on the rod is,

$$\Delta F = F_{original} - F_{resultant}$$
$$= K\left[\delta - (e_E + e_p)\right] - K\left[\delta - (e_E + e_p + e_c)\right]$$
$$= K\left[\epsilon_c\right] .$$

Since $e_c = \epsilon_c L$ and the original length, L, of the specimen is known, e_c can readily be converted to ϵ_c, the creep strain. The change in magnitude of the force is now

$$\Delta F = K\epsilon_c L.$$

It is assumed that $F_{original} \cong \sigma_{yp} \cdot A_{rod}$, and that $F_{resultant} = \sigma \cdot A_{rod}$. The resultant stress in the rod after creep is

$$F_{resultant} = F_{original} - \Delta F,$$

or by substituting from above

$$\sigma A = \sigma_{yp} A - K\epsilon_c L,$$

$$\sigma = \sigma_{yp} - K\epsilon_c L/A .$$

Due to lack of more specific data on primary creep, but within the purpose of this study, use is made of the accepted expression for relation of creep rate to stress, viz.,

$$\dot{\epsilon}_c = B\sigma^n ,$$

Where B is a constant, whose value depends on the metallurgical state of the material (i. e. annealed, cold worked, carburized, etc.) and temperature; and n is an experimentally determined factor used to relate creep rate to load.

The creep strain change in time is, therefore,

$$\frac{d\epsilon_c}{dt} = B\sigma^n .$$

Using the expression for σ previously derived,

$$\frac{d\epsilon_c}{dt} = B(\sigma_{yp} - KL\epsilon_c/A)^n ,$$

which transposes to

$$Bdt = \frac{d\epsilon_c}{(\sigma_{yp} - \frac{KL}{A}\epsilon_c)^n} .$$

Integrating both sides of this equation yields

$$-\frac{BKL}{A}(-n+1)t\Big]_o^t = \left(\sigma_{yp} - \frac{KL}{A}\epsilon_c\right)^{-n+1}\Big]_o^{\epsilon_c} ,$$

which with proper substitution of initial conditions $\epsilon_c = o$ at $t = o$ yields

$$-\frac{BKL}{A}(-n+1)t = \left(\sigma_{yp} - \frac{KL}{A}\epsilon_c\right)^{-n+1} - \left(\sigma_{yp}\right)^{-n+1} ,$$

and after algebraic manipulation becomes

$$\epsilon_c = \frac{A}{KL}\sigma_{yp}\left[1 - \left[1 + \frac{BKL}{A}(n-1)t \cdot \sigma_{yp}^{\,n-1}\right]^{\frac{1}{1-n}}\right] .$$

Using the Binomial Theorem to expand the term,

$$\left[1 + \frac{BKL}{A}(n-1)t \cdot \sigma_{yp}^{\,n-1}\right]^{\frac{1}{1-n}} ,$$

the result of taking the first three terms is,

$$\epsilon_c = \frac{A}{KL}\sigma_{yp}\left[1-\left\{1+\left[\frac{1}{-(n-1)}\frac{BKL}{A}(n-1)t\cdot\sigma_{yp}^{\,n-1}\right]+\left[\frac{\frac{1}{-(n-1)}\left(\frac{1}{-(n-1)}-1\right)}{2!}\left(\frac{BKL}{A}(n-1)t\cdot\sigma_{yp}^{\,n-1}\right)^2\right]\right\}\right] ,$$

which reduces to

$$\epsilon_c = Bt\sigma_{yp}^{\,n}\left[1 - \frac{n}{2}\frac{BKLt}{A}\cdot\frac{\sigma_{yp}^{\,n}}{\sigma_{yp}}\right] .$$

Since $B\sigma_{yp}^{n} = \dot{\epsilon}_c$, the creep rate due to the original force, and $\sigma_{yp}A = F_{original}$, the above expression for $\dot{\epsilon}_c$ reduces further to,

$$\epsilon_c = \dot{\epsilon}_{cF_o} t \left[1 - \frac{n}{2} KLt \cdot \frac{\dot{\epsilon}_{cF_o}}{F_{original}} \right].$$

It should be noted that this expression is deemed sufficiently accurate only for the modified testing machine used in this program, which had holding times of 2 to 3 sec. For longer holding times, the series used previously in this derivation should be expanded.

REFERENCES

1. W. F. Anderson and C. R. Waldron, "High Temperature Strain Fatigue Testing with a Modified Direct-Stress Fatigue Machine," NAA-SR-4051 (September 1959)

2. R. G. Carlson, "Fatigue Studies of Inconel," BMI-1355 (June 1959)

3. D. M. Guy, Jr., "Aloca's Aluminum Powder Metallurgy (APM) Alloys," Aluminum Company of America (March 1959)

4. S. S. Manson, "Behavior of Materials Under Conditions of Thermal Stress," NACA Report 1170 (1954)